Effect of Thermal Nodes Reduction in Wall Connections of the Charge-Handling Furnace Grates on Thermal Stresses

A. Bajwoluk *, P. Gutowski

Mechanical Engineering Faculty, West Pomeranian University of Technology, Szczecin
Al. Piastów 19, 70-310 Szczecin, Polska
* Correspondence contact: e-mail: Artur.Bajwoluk@zut.edu.pl

Abstract

The paper presents FEM approach for comparative analyses of wall connections applied in cast grates used for charge transport in furnaces for heat and thermal-chemical treatment. Nine variants of wall connection were compared in term of temperature differences arising during cooling process and stresses caused by the differences. The presented comparative methodology consists of two steps. In first, the calculations of heat flow during cooling in oil for analysed constructions were carried out. As a result the temperature distributions vs cooling time in cross-sections of analysed wall connections were determined. In the second step, based on heat flow analyses, calculations of stresses caused by the temperature gradient in the wall connections were performed. The conducted calculations were used to evaluate an impact of thermal nodes reduction on maximum temperature differences and to quantitative comparison of various base design of the cast grate wall connection in term of level of thermal stresses and their distribution during cooling process. The obtained results clearly show which solution of wall connection should be applied in cast grate used for charge transport in real constructions and which of them should be avoided because the risk of high thermal stresses forming during cooling process.

Keywords: Cast grates, Heat-resistant castings, Heat treatment equipment, Thermal stress analyses

1. Introduction

Parts of furnace equipment, such as grates and baskets, used for transport of charge during heat treatment and thermo-chemical treatment are exposed to the same conditions as the charge they are carrying. These conditions include significant and rapid temperature changes combined with the impact of furnace chamber atmosphere, additionally enhanced by mechanical loads produced by the charge moving into the furnace chamber and back.

Operation under conditions of rapid temperature changes is associated with the formation of temperature gradients generating thermal stresses which may reach significant values, thus contributing to the destruction of equipment. Several additional factors, including operation in cycles, high temperature, and atmosphere used in the heat-treatment process, may lead to the situation where the initially satisfactory properties of cast steel used for furnace equipment will deteriorate as a result of advancing changes in fatigue behavior [1-6].

As a result of operation under such conditions, castings will degenerate over time and the consequence will be their withdrawal from further use. The most common reasons for such decisions are cracks developing in the grate structure or critical deformation of components.

One of the goals set for the designer of this type of equipment is to develop a structure with geometry ensuring the longest

possible service life of components. This requires the knowledge of both design and operating factors that control this service life and the development of multi-criteria comparative methods for various design solutions to minimize the risk of stress formation [3, 7, 8].

The aim of this article is to show how apparently minor modifications introduced to the design of grate wall connections can significantly reduce the thermal nodes formed in these connections and how it affects the level of thermal stresses arising during rapid cooling.

2. Object of study

The grates used for charge transport in heat-treatment and thermo-chemical treatment furnaces usually operate as individual components or in multi-level sets. In most cases, grates are made of creep-resistant cast steels with high nickel and chromium contents. The geometry of the grate outer contour strictly depends on the dimensions of the furnace chamber in which this grate will be used [1-3]. Examples of grate designs are shown in Figure 1.
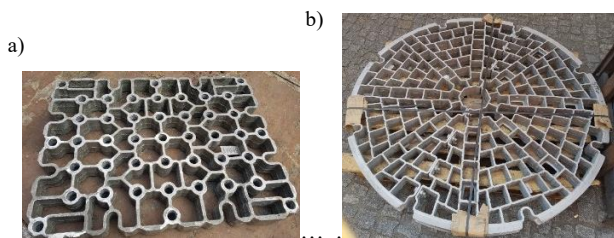

Fig. 1. Examples of accessories for charge transport in furnaces for heat treatment and thermo-chemical treatment

Apart from the overall dimensions and shape of the outer contour, grates differ from each other in the design of their interior space. In the majority of solutions, the interior of the grate comprises interconnected walls, i.e. ribs 6 ÷ 12 mm thick, and empty spaces between them, called sockets. The main task that the properly arranged grate interior is expected to fulfill is to provide sufficiently high strength at the lowest possible weight. In many cases, the grate structure should also ensure proper positioning of the charge and protect it against unexpected movements during transport.

In each operating cycle, the grates experience the same conditions as the heat-treated charge they are carrying. Their operation under conditions of rapid temperature changes generates high stresses which depend, among others, on the thermal properties of the grate material, wall thickness, cooling or heating rate, charge layout on the grate, and uniformity of the temperature distribution in the furnace chamber. During long-term operation of the equipment these stresses lead to the formation of cracks which, by propagating deeper into the material in each subsequent operating cycle, may lead to the withdrawal of grates from further use [1-7].

The areas particularly sensitive to stress formation are grate wall connections where most of the cracks are located (Fig. 2). The reason is the increased wall thickness in these places which results

in temperature changes proceeding more slowly in their surroundings than in the rib joints. Consequently, these places are more exposed to the effect of temperature gradient, mainly because the distance between the center of the connection and casting surface is larger, and an additional direction of the temperature gradient develops between the center of the connection and the joined walls of a regular thickness. Thermal nodes formed in the connections of grate walls are also potential areas where casting defects such as shrinkage porosity or shrinkage cavities may occur. This makes these areas even weaker and can significantly accelerate the damage caused by fatigue process.

Fig. 2. Cracks formed in grate wall connections

Considering the nature of the wall connection areas, the decision on the choice of the best solution and its application in the grate design has a significant impact on the service life of cast grates. Therefore it is important that the decision on the selection of the type of wall connection for practical use in the grate design was supported by careful analysis of the impact it may have on structure stability.

3. Tested variants of connections

Different types of wall connections are used in cast grates. The difference is in the number of connected ribs and angles between them. One of the basic connections formed at the point where the four walls of the grate meet is the *X*-type connection (Fig. 3a). In its most common variant, the joined walls are spaced symmetrically with an angle of 90° formed between them.

In spite of the undeniable advantages of symmetry and the ease of designing the inside space of the grate based on this connection, it is not a good solution for use in structures operating under conditions of rapid temperature changes. This type of connection increases locally the thickness of the wall which during cooling becomes a thermal node, i.e. an area that reacts more slowly to temperature changes than the rest of the connected walls, which unavoidably leads to the formation of additional thermal stresses.

In the currently designed constructions of cast grates, solutions based on less rigid connections of three walls are more popular. It is true that such structures are more complex than standard solutions based on *X*-type connections, but they offer the advantage of reduced thermal nodes and lower stiffness of the connection.

The most popular connection in this group is the *T*-type connection. In this connection, two of the connected ribs constitute one wall of the grate, and the third rib is attached to this wall at an angle of 90° (Fig. 3b). Depending on the specific requirements of a given structure, the third rib may be connected to the wall of the grate at an angle other than 90°. Figure 4 shows commonly used solutions with an angle of 45° (T_{45}) or 60° (T_{60}).
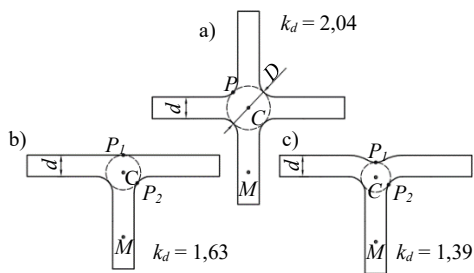
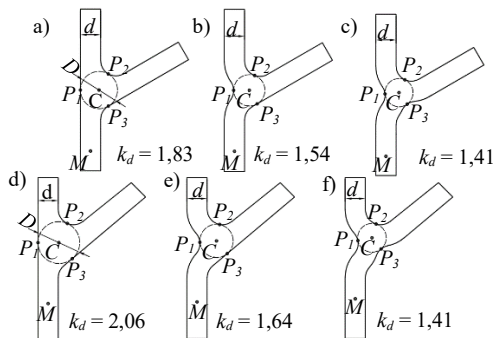Fig. 3. Grate wall connections: a) X, b) T, c) T_m

Fig. 4. Grate wall connections: a) T_{60}, b) T_{60m}, c) T_{60m2}, d) T_{45}, e) T_{45m}, f) T_{45m2}

A measure of the local increase in thickness introduced by individual types of connections is the k_d ratio of the diameter D of the circle inscribed in a given connection to the thickness d of the joined walls ($k_d = D/d$). While in the standard T-type connection, this ratio is lower than in the X-type connection (Fig. 3), in variants with other angles, the value of the ratio may be comparable or even slightly higher (Fig. 4).

To reduce the value of k_d in the T-type connections of the three grate walls, technological recesses, formed by the removal of a certain volume of material from the wall connection (on the side of the surface formed by two parallel ribs), are provided. Variants of such modified connections are shown in Figures 3c, 4b, 4e and are designated by the symbols T_m, T_{45m} and T_{60m}, respectively. Figures 4c and 4f also show variants of these connections with an additional recess made between the ribs forming an obtuse angle. They are designated as T_{60m2} and T_{45m2}, respectively.

From the numerical calculations performed in the conducted analysis it follows that technological recesses have a great impact on the improvement of heat flow in the vicinity of wall connections during cooling, affecting also in a beneficial way the distribution of stresses and reducing their maximum value in some directions.

3. Heat flow analysis

Numerical analysis of the influence of the adopted type of wall connection on the heat flow during rapid cooling was based on FEM models of the designed connection. In the analysis, the initial temperature of whole finite element mesh was assumed to be $T_0 = 900°C$, while quenching oil at a temperature $T_q = 20°C$ was used as the cooling medium.

It was also assumed that the tested components are made of cast steel grade 1.4849 (GX40NiCrSiNb38-19). According to the PN-EN 10295: 2004 standard [9], the specific heat of this material is $C_a = 500\ J / (kg \cdot K)$. Its thermal conductivity λ_a was modeled with a linear function (Fig. 5), based on the data provided by the above mentioned standard.
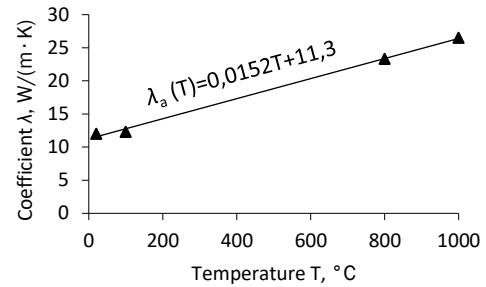

Fig. 5. Thermal conductivity of cast steel 1.4849 plotted as a function of temperature adopted in calculations

Another assumption made in the studies was that the heat exchange with the environment is by free convection through the wall surfaces in contact with the surrounding cooling medium. The calculations were based on the experimentally established, simplified function of relationship between the heat transfer coefficient h and temperature [10], presented in Figure 6. This relationship allows for the change in the condition of the quenching oil, which at elevated temperatures should be treated as a boiling-evaporating liquid characterized by a much higher value of this coefficient than the same liquid at lower temperatures.
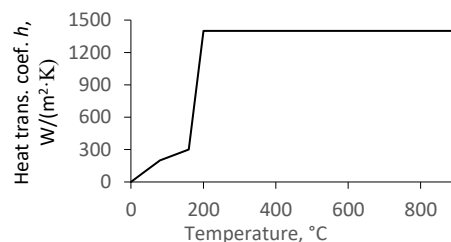

Fig. 6. Heat transfer coefficient vs temperature relationship adopted in studies

Models of connections were developed in Solidworks 2019 and were next imported to Midas NFX 2017 software, where the heat flow in the examined models during cooling was calculated using transient heat flux module. The assumed height of the connections was 50 mm with the wall thickness of 8 mm. Simulation analysis covered a 15 second period of the cooling process. The adopted calculation step was 0.25 s.

As a result of these calculations, temperature distributions in the examined connections were determined as a function of time. Examples of temperature distributions in selected connections after 1 second and 5 seconds of the cooling time are presented graphically in Figure 7.

In the analysis of the heat flow effect on stresses arising in a given structure, very important are changes in temperature differences that occur in various areas of the structure with the

resulting formation of temperature gradients. On the sketches of the examined connections shown in Figures 3 and 4, points C, P_i and M are marked. Point C is the center of the circle inscribed in a given connection, points P_i lie on the contact line between the circle and the surface, while point M lies in the middle of the connected walls at a distance $2.5d$ from the center of the connection, i.e. in the area where the heat flow disturbances caused by the presence of the connection are already negligibly small. These points indicate the directions in which the temperature differences arising in the connections are examined.
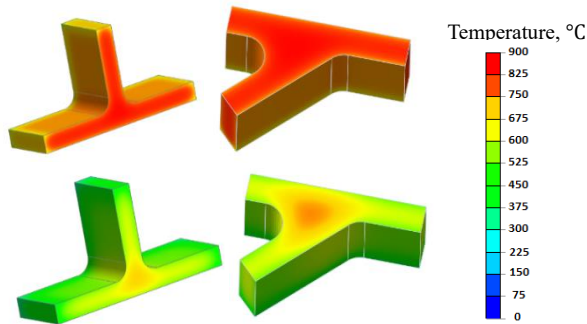

Fig. 7. Temperature distribution on horizontal cross-section of connections T and T_{45} after cooling time: a) 1s, b) 5s

Figure 8 shows changes in temperature difference determined numerically for the examined connections in direction C-P_{max}, while Figure 9 shows the same comparison for direction C-M. In either case, the waveforms obtained for connection X were used as a reference. Tables 1 and 2 show the greatest temperature differences obtained for various directions, where Table 1 lists the results obtained for connections without technological recesses and Table 2 gives values obtained for modified connections, i.e. with recesses. The values in parentheses represent the results obtained for asymmetrical connections at different points P_i.

It is easy to notice that in directions C-P_i, the maximum temperature differences determined for connections from the T group, i.e. without technological recesses, are higher than it would appear from the comparison of their D/d ratio with connection X

Table 1.
Maximum temperature differences in wall connections without technological recesses

Connection	k_d	ΔT_{max}^{CP} [°C]	ΔT_{max}^{CM} [°C]
X	2.04	129.4	173.8
T	1.63	131.8 (107.5)	115.3
T_{60}	1.83	140.6 (123.4; 113.2)	135.6
T_{45}	2.06	167.3 (163.2; 132.7)	187.2

Table 2.
Maximum temperature differences in wall connections with technological recesses

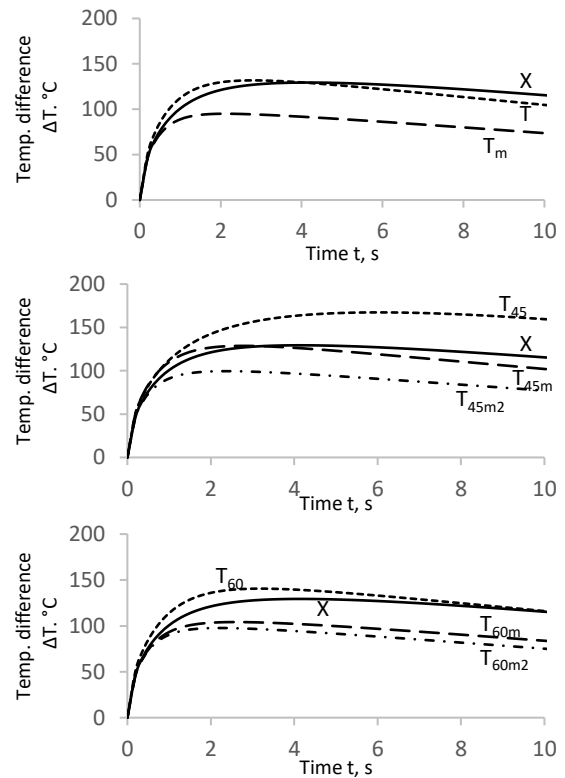| Connection	k_d	ΔT_{max}^{CM} [°C]	ΔT_{max}^{CM} [°C]
T_m	1,39	101,1 (97.7)	79.3
T_{45m}	1,64	128.4 (105.9; 103.9)	112.2
T_{45m2}	1,41	98.4 (96; 93.6)	79.2
T_{60m}	1,54	112.6 (104; 100)	97.2
T_{60m2}	1,41	97.7 (97.3; 94)	78.6

Fig. 8. Changes in temperature difference for direction C-P

In connection T, despite the reduced thermal node, the maximum temperature difference in one of the analyzed directions is higher than in connection X.

In connection T_{60}, despite its k_d value lower than in connection X, because of the asymmetry of the connection, temperature differences between the center and the surface are greater than in the reference connection. The situation is similar in connection T_{45} where, despite the k_d value approaching that obtained for connection X, the asymmetric arrangement of ribs accounts for much higher, i.e. by about 29%, maximum temperature differences in direction C-P.

In all connections with technological recesses, the maximum temperature differences during cooling assumed lower values than in their unmodified counterparts. Careful analysis of the data in Table 2 shows that technological recesses used as a means of reducing thermal nodes formed in the grate wall connections were much more effective in reducing the maximum temperature differences in direction C-M (connection center - wall center) than in direction C-P. For example, in the T-type connection, the introduction of a recess lowered the maximum temperature difference by about 11.6% for direction C-P and by about 31.2% for direction C-M. Similar dependencies were obtained for the remaining examined connections in which technological recesses were made.

In the case of connections with an additional modification, the second recess introduces further reduction in temperature differences that occur during cooling. The numerical results obtained for these variants are comparable with the results obtained for connection T_m.
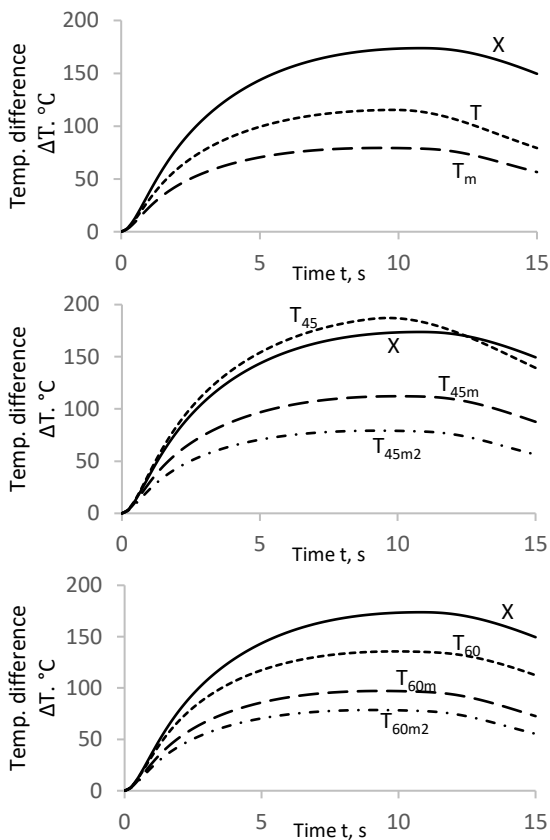
Fig. 9. Changes in temperature difference for direction C-M

4. Stress distribution analysis

The results obtained in the heat flow analysis were used as input data in the analysis of stresses arising in the examined connections. The first step in the computational methodology was to determine for each of the connections the time t_{max}^{CP} and t_{max}^{CM} after which the temperature difference in a given direction assumed its highest value. In each case, in the stress analysis, the load was the temperature change from the initial $T_0 = 900°C$ to the distribution after time t_{max}, when in the examined wall connection, the temperature difference between the central point C and the examined point P or M was the greatest.

In the calculations, an elasto-plastic model of the material with non-linear hardening was adopted, in which the true tensile curve was approximated with several straight line segments characterized by different values of the strain-hardening modulus E_{ai}. In the calculations made for austenite, the following experimental mechanical properties were adopted: thermal expansion coefficient $\alpha_a = 17.7 \cdot 10^{-6}$ 1/K, Poisson number $v_a = 0.253$, Young's modulus $E_a = 1.73 \cdot 10^5$ N/mm², yield stress $R_e = 208$ N/mm², and strain-hardening modulus $E_{a1} = 4.09 \cdot 10^3$ N/mm² for the case of exceeded yield strength.

As a result of numerical calculations, stress distributions were determined for both examined cases. Sample distributions of reduced stresses, determined in accordance with the Huber-Mises

hypothesis on the cross-section of connection T after the time t_{max}^{CP} and t_{max}^{CM}, are presented graphically in Figure 10.
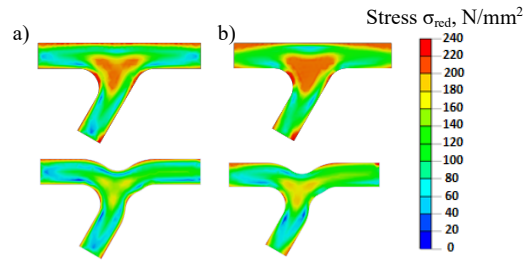

Fig. 10. Stress distribution on cross-section of connections T_{60} and T_{60m2} under loading with temperature distribution over time: a) t_{max}^{CP}, b) t_{max}^{CM}

The stress distributions σ_{red} obtained for the examined connections in directions C-P and C-M before and after modification are shown in Figures 11 and 12, respectively. Figure 11 shows the stress distribution in direction C-P under conditions of loading with temperature distribution over time t_{max}^{CP}, while Figure 12 shows the stress distribution in direction C-M under conditions of loading with temperature distribution over time t_{max}^{CM}. As in the case of changes in temperature differences, the distributions obtained for connection X were used as a reference.
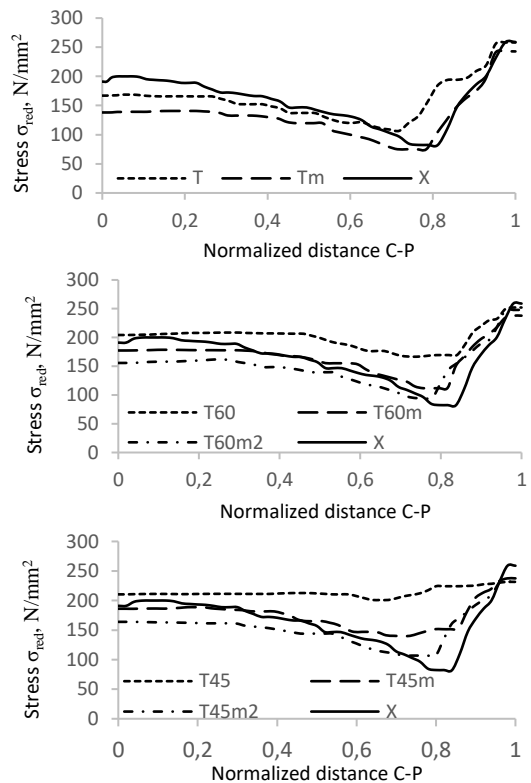

Fig. 11. Stress distribution σ_{red} obtained for direction C-P over time t_{max}^{CP}
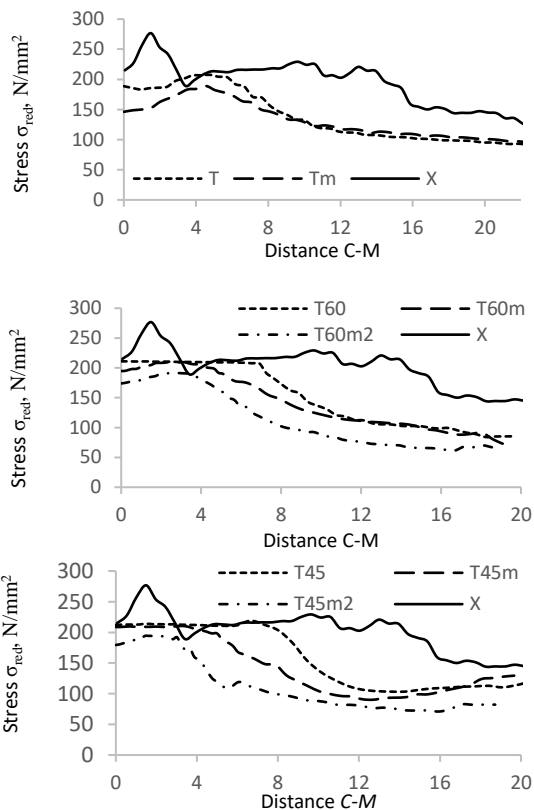
Fig. 12. Stress distribution σ_{red} obtained for direction C-M over time t_{max}^{CM}

The diagrams show that in all connections, the use of technological recesses significantly influenced the obtained stress distributions for both directions C-P and C-M.

In the case of direction C-P and time t_{max}^{CP}, the stresses are definitely lower in the connections with recesses, but in the case of very high stresses generated at this stage of cooling in the grate surface and subsurface zone, the differences between the variants with and without technological recesses are so insignificant that it cannot be claimed that the introduced recesses have really affected the stress value.

The differences in stresses determined for the variants with and without technological recesses are more visible in the stresses determined for direction C-M under conditions of loading with temperature distribution over time t_{max}^{CM} (Fig. 12). Analyzing the waveforms plotted in this drawing it is clear that, owing to the reduced value of k_d in the modified connections, it was possible to significantly reduce the level of stresses and the area of the occurrence of high stresses adjacent to the wall connections.

Attention deserves the fact that for this particular direction, a very large drop in stresses (up to 50%) has occurred in the connections with double technological recesses.

Numerical calculations presented in this study allowed for a quantitative comparison of various designs of the wall connections in cast grates used for the transport of charge in heat treatment furnaces to better understand their role in the occurrence of heat flow disturbances and resulting thermal stresses.

On base of the obtained results of performed numerical analyses the following conclusions can be formulated:

1. From the analysed variants of constructional solutions connections T_{45}, X and T_{60} present the worst results and they should not be used in grates exposed to rapid temperature changes;
2. The proposed technological recesses have significantly impact on reduction of maximum temperature differences and stress distribution on analyzed directions;
3. Thanks to proposed recesses similar results of stress distribution analyses for different geometry shape of wall connection were obtained

The obtained results can be used not only for cast grates but also for others constructions worked under conditions of rapid temperature changes.

References

[1] Lai, G.Y. (2007). *High-Temperature Corrosion and Materials Applications*. ASM International.

[2] Davis, J.R. (Ed.). (1997). Industrial Applications of Heat-Resistant Materials. In Davis, J.R. (Eds.), *ASM Specialty Handbook - Heat-Resistant Materials* (pp. 67-85). ASM International.

[3] Piekarski, B. (2012). *Creep-resistant castings used in heat treatment furnaces*. Szczecin: West Pomeranian University of Technology Publishing House. (in Polish).

[4] Ul-Hamid et al. (2006). Failure analysis of furnace tubes exposed to excessive temperature. *Engineering Failure Analysis*. 13(6), 1005-1021. DOI: 10.1016/j.engfailanal.2005.04.003.

[5] Reihani, A., Razavi, S.A., Abbasi, E. et al. (2013). Failure Analysis of welded radiant tubes made of cast heat-resisting steel. *Journal of failure Analysis and Prevention*. 13, 658–665. DOI: https://doi.org/10.1007/s11668-013-9741-y.

[6] Piekarski, B. (2010). Damage of heat-resistant castings in a carburizing furnace. *Engineering Failure Analysis*. 17(1), 143-149. DOI: 10.1016/j.engfailanal.2009.04.011.

[7] Nandwana, D., et al. (2010). Design, Finite Element analysis and optimization of HRC trays used in heat treatment process. In World Congress on Engineering 2010, June 30 - July 2, 2010 (pp. 1149-1154). London, U.K.: Newswood Limited.

[8] Sandeep, K., Ajit, K. & Mahesh, N.S. (2012). Improving productivity in a heat treatment shop for piston Pins. *SASTECH Journal*. 11(2), 38-46.

[9] Standard PN-EN 10295: 2004. Heat resistant steel castings.

[10] Bajwoluk, A. & Gutowski, P. (2019). Thermal stresses in the accessories of heat treatment furnaces vs cooling kinetics. *Archives of Foundry Engineering*. 19(3), 88-93, DOI: 10.24425/afe.2019.127146.